Plane-waves at the interface between two-dimensional cyclic Lotka-Volterra and May-Leonard systems

M. Lazarus Arnau
PHYS 4316 Modern Experimental Physics

May 10, 2020

Abstract

The spatially extended May-Leonard model for cyclic competition is known to demonstrate (quasi-)stable spatio-temporal patterns in the form of spiral-waves. We investigate how competition between the May-Leonard model and cyclic Lotka-Volterra models governing different spatial regions of a two-dimensional system influences the formation of spiral-waves. To this end we employ a lattice-based Monte-Carlo simulation. We report disruption of the spiral-waves near the interface for certain mobility rates in the cyclic Lotka-Volterra region. We quantify the behavior of these plane-waves by computing the vertical auto-correlation functions. We also report a significant decrease in local population density near the interface.

1 Introduction

Many systems across nature follow a cyclic, or Rock-Paper-Scissors (RPS) like, paradigm of competition. As such, cyclic competition models have been used to describe the evolutionary dynamics and noise-induced pattern formation in such systems (e.g. certain species of side-blotched lizards[6], in-vitro experiments performed on colonies of *E. coli* bacteria [5], and the Belousov-Zhobatinsky reaction [2]). Two variations of three-species competition models that have been extensively studied are the May-Leonard model and cyclic Lotka-Volterra model [1]. Of note is that in its spacially extended variant the May-Leonard model has been shown to demonstrate noise-induced spatio-temporal pattern formation whereas the cyclic Lotka-Volterra model does not [1].

Our goal in this paper is to investigate how competition between the cyclic Lotka-Volterra and May-Leonard models impacts the spatio-temporal dynamics demonstrated by the May-Leonard model. To that end, we describe a stochastic spatially-extended lattice based system which is governed by the two models on different spatial regions of the lattice. We implement a Monte-Carlo simulation of this system and report the results of the simulations. We describe the formation of plane-waves at the interface between the two models and quantify their formation by coputing the vertical auto-correlation function. We also report a drop in local population density near the interface.

2 Our system

2.1 The May-Leonard and Cyclic Lotka-Volterra models

The May-Leonard model (MLM) and cyclic Lotka-Volterra models both describe systems in which the population obeys a cyclic (or Rock-Paper-Scissors) competition scheme. Individuals are thus modeled as particles which can be one of three species, $S \in \{ S_1, S_2, S_3 \}$ with the cyclic symmetry $S_4 = S_1$. These particles are equipped with different reactions. The original May-Leonard (MLM) model defines two reactions, predation and reproduction:

$$S_n + S_{n+1} \to S_n + \emptyset \qquad \text{with rate } \sigma \tag{1}$$

$$S_n + \emptyset \to S_n + S_n \qquad \text{with rate } \beta \tag{2}$$

The cyclic Lotka-Volterra model (CLVM) defines a single predation and reproduction reaction:

$$S_n + S_{n+1} \to S_n + S_n \qquad \text{with rate } \zeta \tag{3}$$

A particle can move from its current node $\boldsymbol{x}$ to one of its nearest neighbors $\boldsymbol{x'}$ via a mobility process

$$X_{\boldsymbol{x}} + Y_{\boldsymbol{x'}} \to Y_{\boldsymbol{x}} + X_{\boldsymbol{x'}} \qquad \text{with rates } \delta_{\text{CLV}} \text{ and } \delta_{\text{ML}} \tag{4}$$

Where $X \in \{ S_1.S_2, S_3 \}$ and $Y \in \{ \emptyset, S_1.S_2, S_3 \}$. It is common to have two different reactions for pair-exchanges (between active nodes) and diffusion (in to empty nodes) [1]. By combining the two processes we are merely simplifying to the case in which the pair-exchange rate is equal to the diffusion rate.

Mean field analysis of a pure CLVM system reveals a marginally stable reactive fixed point of $\boldsymbol{\rho}^*_{\text{CLV}} = (\rho/3, \rho/3, \rho/3)$ where $\rho = \rho_1(t) + \rho_2(t) + \rho_3(t)$ is a conserved quantity[4]. The CLVM also admits three unstable two-species extinction absorbing states [4]. Similar analysis of the MLM reveals a reactive fixed point $\boldsymbol{\rho}^*_{\text{ML}} = \frac{\beta}{3\beta+\sigma}(1, 1, 1)$ as well as four unstable absoring states $\boldsymbol{\rho} = (1, 0, 0)$, $(0, 1, 0)$, $(0, 0, 1)$, and $(0, 0, 0)$ [3].

The spatially extended versions of these two models exhibit drastically different behaviors. The MLM will produce distinctive spiral waves whose size ℓ is determined by δ_{ML} [3]. These waves are quasi-stable, remaining present for very long time scales as long as the diffusivity of the system $D = \delta_{\text{ML}}/M^2$ (where M is the side length of the lattice) stays under a critical threshold D_c at which point the probability with which the system reaches one of the two-species extinction absorbing states rapidly approaches 1. The CLVM, while it will also maintain a quasi-stable stationary state around the coexistence fixed point it does not show any form of spatial pattern formation[1].

2.2 Monte-Carlo simulation

We simulate our system on a lattice of size $N = M \times M$ with periodic boundary conditions. In mixed model simulations, the lattice is governed primarily by the ML model reactions (1, 2, 4) with the CLV model reactions (3) and (4) being imposed on the region $\{ (x, y) : 0 \leq x \leq W \}$ where a width of $W = 64$ lattice nodes is normally used. This makes those interface between the CLVM region and the ML region a continuous vertical line that wraps around the toroidal

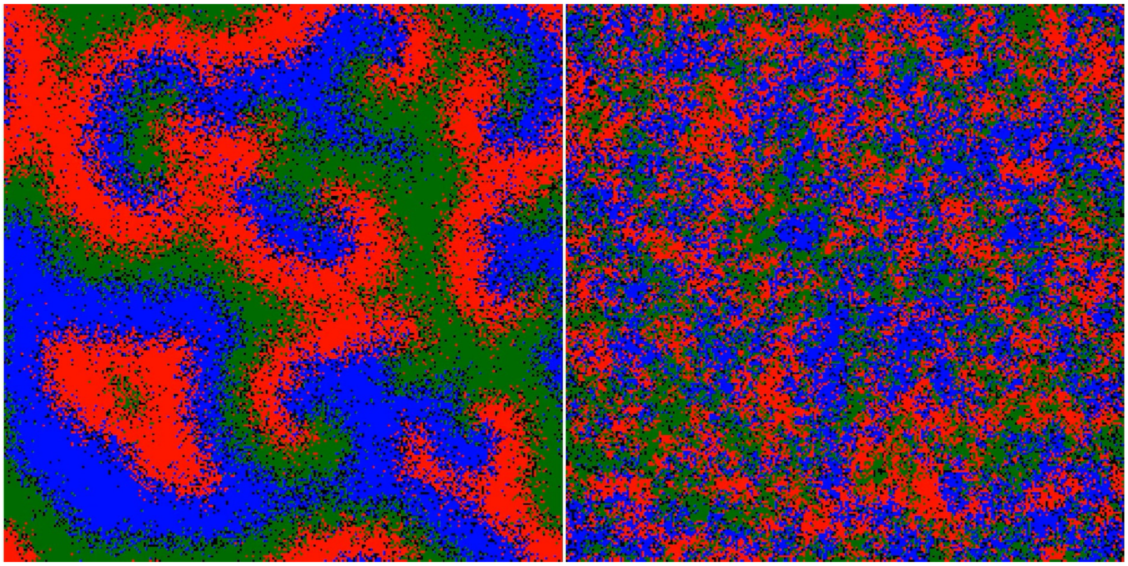

(a) (b)

Figure 1: Snapshots of typical behavior of the spatially extended May-Leonard (a) and cyclic Lotka-Volterra (b) models on a simulation of a 256×256 lattice. The rates used in the simulations for these images are $\sigma = \beta = \zeta = 1.0$, $\delta_{\mathrm{ML}} = 5.0$, and $\delta_{\mathrm{CLV}} = 1.25$

lattice like a ring. This allows us to calculate quantities averaged over columns parallel to the interface, the benefit of which will be apparent.

The lattice is initialized to random, homogeneous initial conditions with $\boldsymbol{\rho} = (0.3, 0.3, 0.3)$. At each simulation step an active particle is selected by drawing random lattice nodes $\boldsymbol{x}$ until a nonempty node is selected. Then one of the four nearest neighbors $\boldsymbol{x}'$ is selected at random. A reaction is then chosen at random from the model governing $\boldsymbol{x}$. The probability with which a reaction is chosen is given by its rate divided by the sum of all rates defined by the given model. So for instance, the probability that predation is chosen if $\boldsymbol{x}$ is in the ML region of the lattice is $\frac{\sigma}{\sigma+\beta+\delta_{\mathrm{ML}}}$. If the reaction chosen isn't possible with the chosen nearest neighbor the time step is still counted and a new $\boldsymbol{x}$ and $\boldsymbol{x}'$ are chosen. We define one Monte-Carlo step (MCS) to be the amount of time it takes on average for every particle to have an opportunity to react or migrate. Each MCS is thus composed of N infinitesimal simulation steps.

Unless noted otherwise the simulations are performed on a 512×512 lattice with rates $\sigma = \beta = \zeta = 1.0$, $\delta_{\mathrm{ML}} = 5.0$, and $\delta_{\mathrm{CLV}} = 1.25$.

3 Monte Carlo simulation results

3.1 Plane-wave characterization

We simulate the two-model system with $\delta_{\mathrm{ML}} = 5.0$ as at that value the pure ML model produces well defined spiral waves that are small enough that several spirals fit on a 512×512

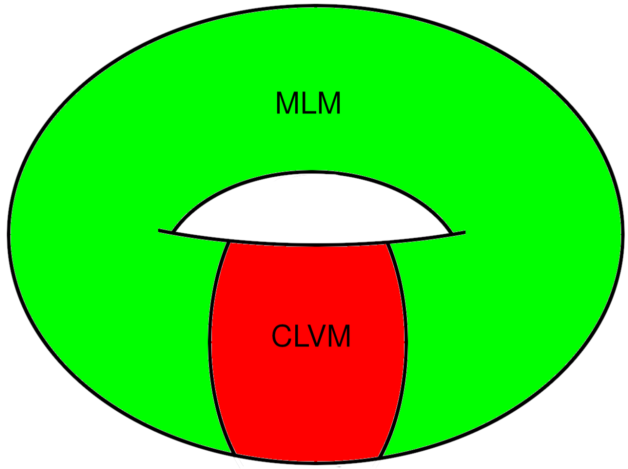

Figure 2: A schematic diagram illustrating the topology of the lattice and the ring shaped CLVM patch

lattice. When the CLVM and MLM are implemented on the same lattice, for values of δ_{CLV} below a certain value, the system displays a disruption of the spiral-wave patterns in the form of plane waves which travelaway from the interface. We observe that, with $\delta_{\mathrm{ML}} = 5.0$, the plane waves begin to disappear at $\delta_{\mathrm{CLV}} = 25.0$. The presence of these plane-waves is determined visually. We further quantify and characterize and quantify their behavior by calculating the vertical correlation length for each column of the system.

We calculate the vertical two-point autocorrelation function for species j at time t

$$C_{jj}(r, x, t) = \frac{1}{M} \sum_{k=1}^{M} n_j(x, k, t) n_j(x, k + r, t) - \rho_j(x, t)^2 \tag{5}$$

where $n_j(x, y, t)$ is the population of species j at the node $\boldsymbol{x} = (x, y)$ and $\rho_j(x, t) = M^{-1} \sum_{k=1}^{M} n_j(x, k, t)$ is the population density of species j in column x of the lattice. Because of the cyclic symmetry inherent to RPS competition schemes, we only calculate C_{jj} for $j = 1$. We calculate $\langle C_{jj}(r, x) \rangle$ by averaging $C_{jj}(r, x, t)$ across 256 measurements taken every 4 MCS starting at $t = 3000$ MCS (by which point the system has reached a (quasi-)steady state). $\langle C_{jj}(r, x) \rangle$ is then finally averaged over 50 simulation runs. Using $\langle C_{jj} \rangle$ we obtain the vertical correlation length $L(x)$ where $L(x)$ is defined the least R for which $\langle C_{jj}(R, x) \rangle$ is less than some threshold ϵ (here taken to be 10^{-2}).

For values of δ_{CLV} for which plane waves are present (figure 4 (a), and the red green and blue lines on figure 4 (b)) we observe an increase in $L(x)$ near the interface which returns to the MLM charcteristic length within 56-100 lattice sites of the interface. Notably, even for values of δ_{CLV} for which plane waves were not observed (the black and magenta plots in figure 4 (b)) we still see an increase in correlation lengths near the interface which disappears more quickly. Finally, we also observe an increase in $L(x)$ in CLV region within approximately 15 lattice sites of the interface for values of δ_{CLV} above 20.0.

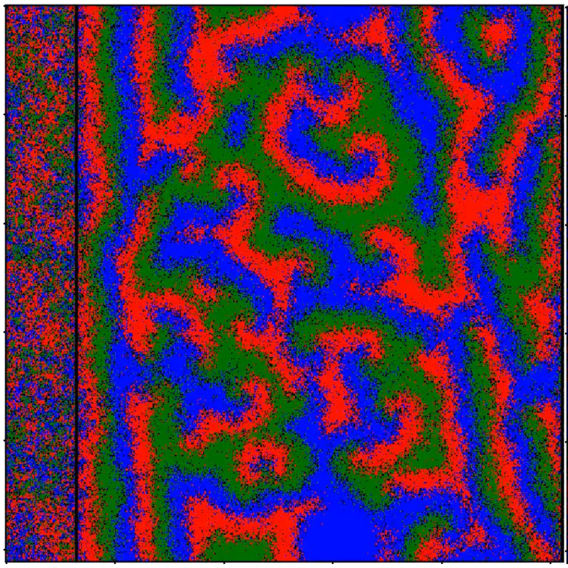

(a) $\delta_{\mathrm{CLV}} = 2.5$

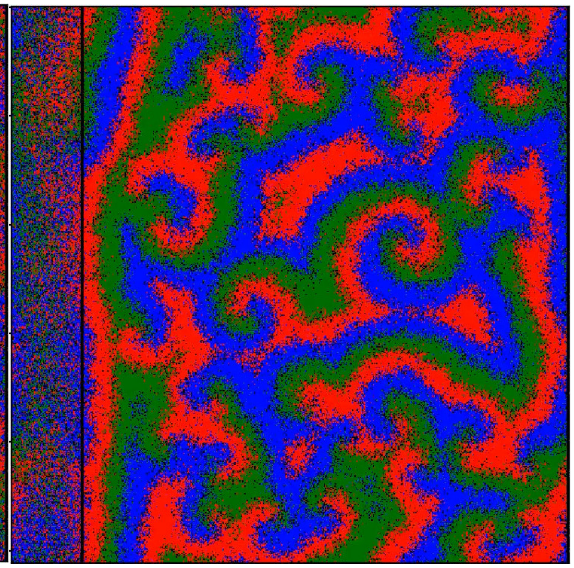

(b) $\delta_{\mathrm{CLV}} = 24.0$

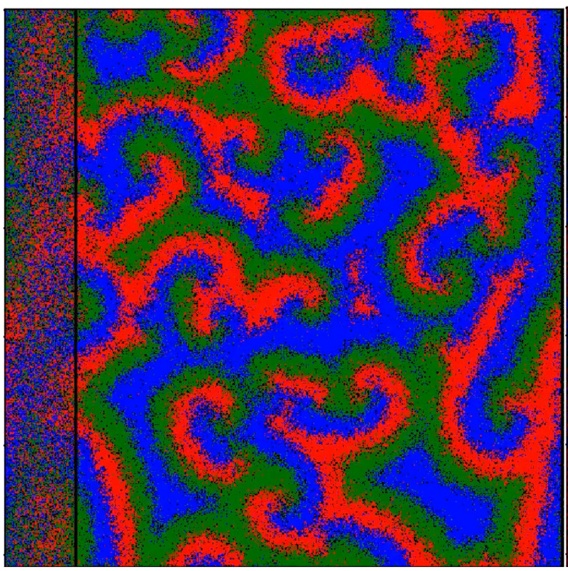

(c) $\delta_{\mathrm{CLV}} = 25.0$

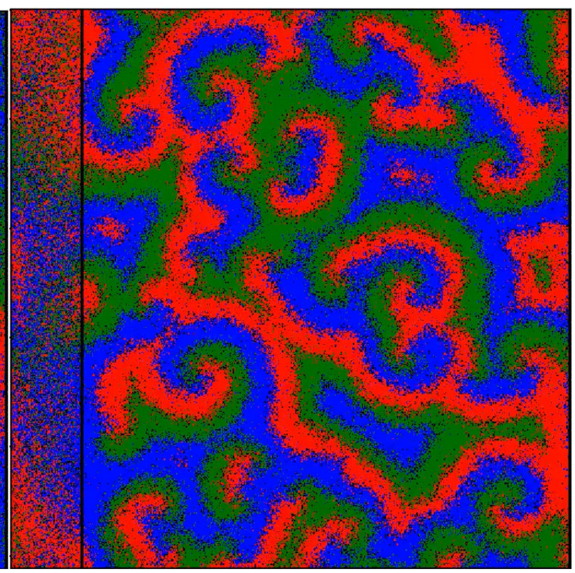

(d) $\delta_{\mathrm{CLV}} = 30.0$

Figure 3: Snapshots of combined CLVM and MLM systems on 512×512 lattice with different values of δ_{CLV}. The thick black line indicates the interface between the CLV and ML regions of the lattice.

3.2 Population density

It is established that spatially extended ML systems starting from randomized initial conditions exhibit an initial decline in global population density before spiral waves form, at which point predation is only possible at the border between species domain boundaries [3]. This causes the carrying capacity of the spatially-extended MLM to be greater than that of

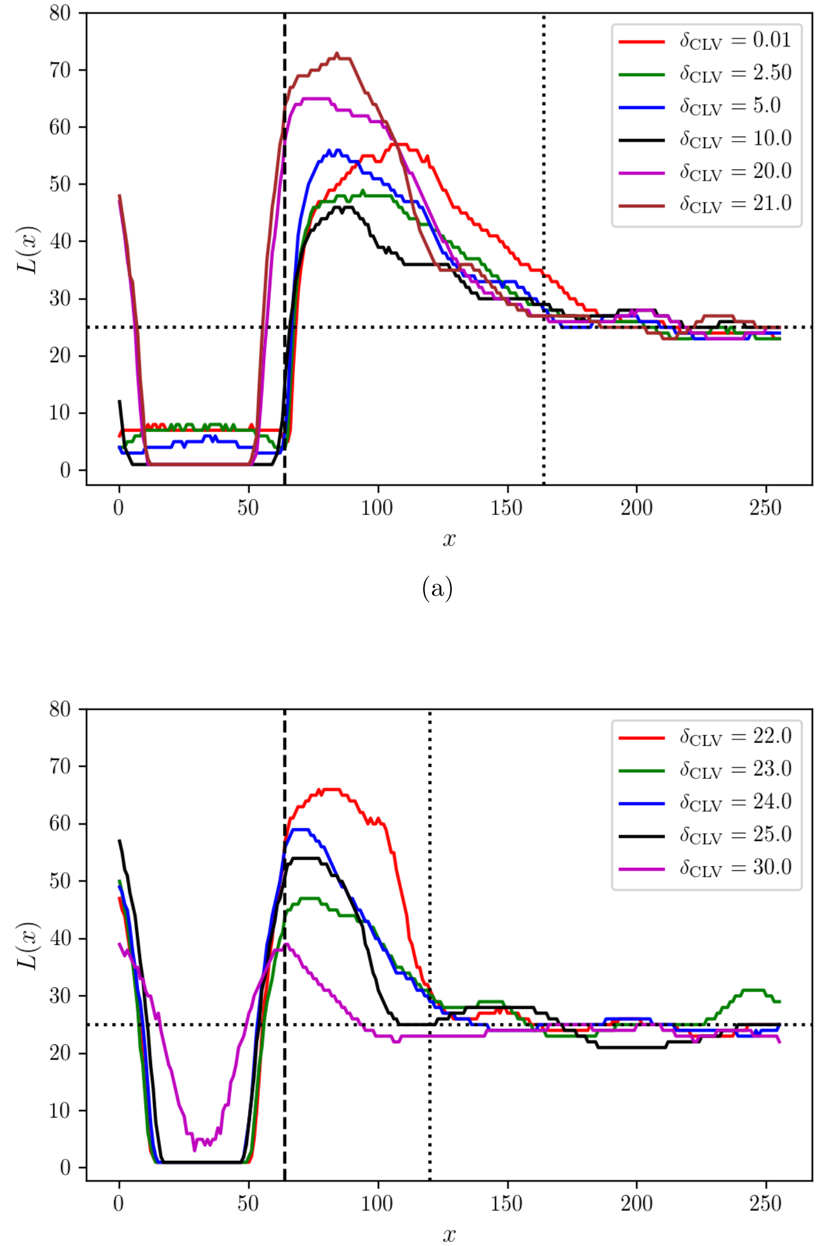

(a)

(b)

Figure 4: Vertical correlation lengths $L(x)$ calculated for different values of δ_{CLV}. The vertical dashed line indicates the interface between the CLV and ML regions of the lattice at $x = 64$ and the vertical dotted lines are at $x = 164$ and $x = 120$ in (a) and (b) respectively.

a "well mixed" system. We replicate this result by computing the global population density $\rho(t) = N^{-1} \sum_{j=1}^{3} \sum_{k=1}^{M} \sum_{l=1}^{M} n_j(l,k,t)$ for simulations of pure ML systems on a 256×256 lattice (figure 5).

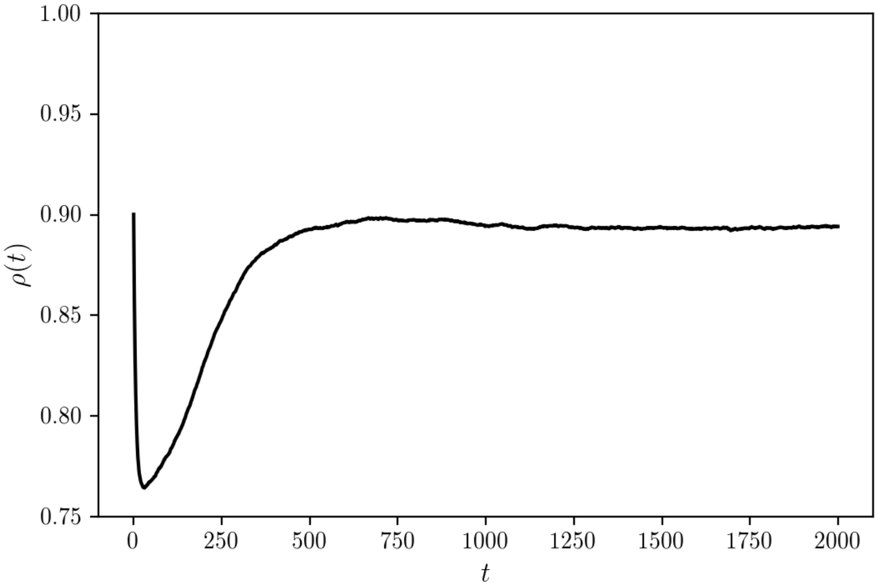

Figure 5: Global population density calculated for simulations of pure-ML systems. Averaged over 50 simulations.

We compute the vertical net population density $\rho(x,t) = M^{-1}\sum_{j=1}^{3}\sum_{k=1}^{M} n_j(x,k,t)$. $\rho(x)$ is then calculated by averaging $\rho(x,t)$ across 256 measurements taken every 4 MCS starting at $t = 3000$ MCS. $\rho(x)$ is then averaged over 50 simulation runs. We observe a decrease in vertical population density near the interface (figure 6) indicating that there is an increase in predation in ML region near the interface. For low values of δ_{CLV} (the red plot in figure 6 (a)) the drop in local density is further enhanced by a net imbalance in migration between the two regions as indicated by the increase in density of the CLV region near the interface. Note that the net density at the interface is less then both the initialized denisty and the ML carrying capacity. This suggests that there is still some sort of "well mixing" effect allowing for increased predation at the interface despite the enhanced correlation length displayed in figure 4.

4 Discussion

In this paper, we demonstrate the appearance of plane-waves near the interface of mixed CLVM-MLM systems. We report an overall increase in vertical correlation lengths near the interface across all values of δ_{CLV} tested. As the value of δ_{CLV} is increased, the maximum distance from the interface at which the system still displays an increased correlation length decreases. This suggests that, while there is still some disruption of the spiral-wave formation occuring for higher values of δ_{CLV}, it gives way quickly to the more stable spiral-waves. Furthermore, we report a decrease in local population density near the interface indicating a local increase in predation. Overall, these results suggest localized periodic mixing as a means by which to disrupt otherwise stable pattern formation in the MLM.

References

[1] U. Dobromasyl, M. Mobilia, M. Pleimling, and U. C. Täuber. Stochastic population dynamics in spatially extended predator prey systems. *J. Phys. A: Math. Theor.*, 51(6), 2018.

[2] I. R. Epstein and K. Showalter. Nonlinear chemical dynamics: oscillations, patterns, and chaos. *The Journal of Physical Chemistry*, 100(31):13132–13147, 1996.

[3] Q. He, M. Mobilia, and U. Täuber. Coexistence in the two-dimensional May-Leonard model with random rates. *Eur. Phys. J. B*, 82:97–105, 2011.

[4] Q. He, U. C. Täuber, and R. K. P. Zia. On the relationship between cyclic and hierarchical three-species predator-prey systems and the two-species Lotka-Volterra model. *Eur. Phys. J. B*, 8(141), 2012.

[5] B. Kerr, M. Riley, M. Feldman, and B. Bohannan. Local dispersal promotes biodiversity in a real-life game of rock-paper-scissors. *Nature*, 418:171–174, 2002.

[6] B. Sinervo and C. Lively. The rock-paper-scissors game and the evolution of alternative male strategies. *Nature*, 380:240–243, 1996.

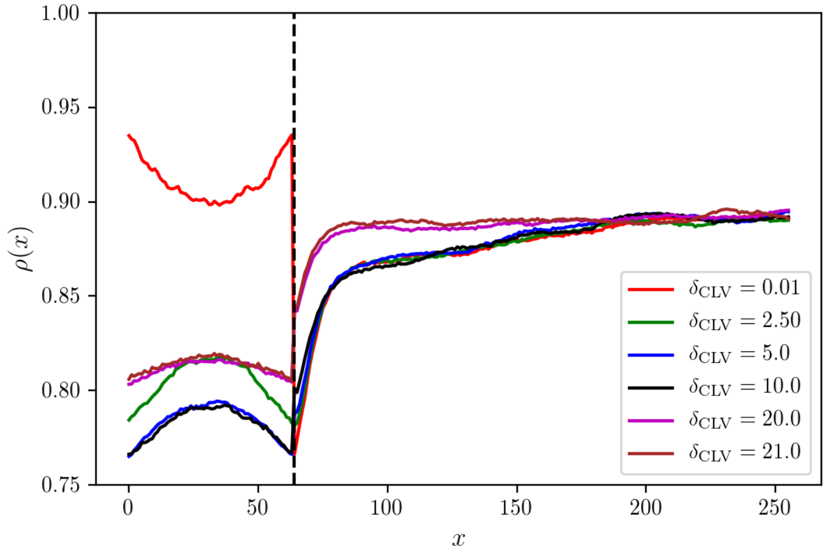

(a)

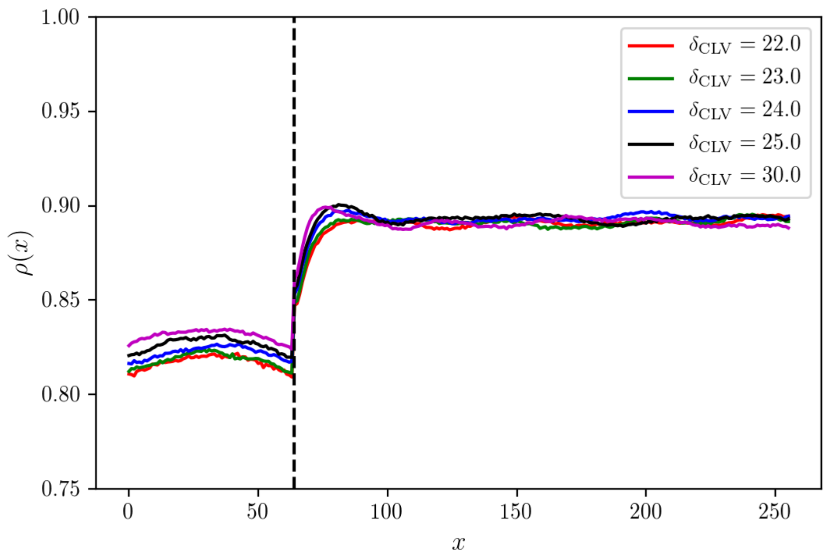

(b)

Figure 6: Vertical net population densities $rho(x,t)$ calculated for different values of δ_{CLV}. The vertical dashed line indicates the interface between the CLV and ML regions of the lattice at $x = 64$.